# ENERGETIC BEHAVIOUR OF A SOLAR THERMAL SYSTEM PRODUCING DOMESTIC HOT WATER AND PREHEATING THE VENTILATION AIR

**Patricia Carbajo Jiménez[1,2], Antoine Leconte[2], Gilles Fraisse[1], Ophélie Ouvrier Bonnaz[2], Etienne Wurtz[2]**

[1]Univ. Grenoble Alpes, Univ. Savoie Mont Blanc, CNRS, LOCIE, 73000 Chambéry, France.
[2]Univ. Grenoble Alpes, CEA, LITEN, INES, 73375 Le Bourget-du-Lac, France.

**Abstract**

As a result of the evolution of the thermal regulation in Europe, buildings are better isolated and more airtight, thereby reducing their heating needs. Efficient systems from the energetic point of view, using preferably renewable sources, must cover the new distribution of needs. Indeed, domestic hot water (DHW) becomes a more important load than space heating in residential buildings. In this context, solar thermal systems are appropriate for supplying a significant part of the heat demand in energy efficient housing. Thus, this paper focuses on an innovative solar thermal system producing DHW and preheating the ventilation air. A co-simulation between Dymola (Modelica language) and EnergyPlus forecasts the energy performance of the system in a low-energy individual house for different French cities. The results show an improved collector efficiency as well as a higher solar productivity in comparison to a classical solar domestic hot water system. Although energy savings are achieved for the majority of the studied climates with the studied system, a different control strategy may be interesting in order to improve the distribution of the collected solar energy. To this end, a parametric analysis provides some clues for increasing the energy performance of the innovative system when modifying the design and control parameters.

*Keywords:* solar thermal system, air preheating, DHW, low-energy building, Modelica, EnergyPlus, FMU

## 1. Introduction

The building sector represents a major axis of the European energetic policy. Indeed, it is responsible for almost 40% of the final energy consumption and for about 36% of the greenhouse emissions in the European Union (European Commission, 2013). Consequently, many efforts have been done in order to decrease energy consumption and, at the same time, increase the use of renewable energy sources in buildings.

For existing residential buildings, about 55% of the final energy demand is used for comfort heat (space and water heating) (IEA-ETSAP and IRENA, 2015). In recent high-performance houses, space heating needs have been considerably reduced by improving the building envelope (isolation and air-tightness) and by increasing passive gains during the cold season (Ionescu et al., 2015). Thus, air renewal losses constitute an important part of the space heating needs in efficient buildings and can also be decreased by using heat recovery systems or natural thermal sources for fresh air conditioning. In this context, domestic hot water (DHW) needs become a large portion of the heat demand in buildings and may even be more important than space heating needs (Faninger, 2010).

Since solar thermal systems are a mature and competitive technology for DHW production (IEA, 2012), this paper studies an innovative solar domestic hot water system which can also preheat the supplied fresh air. Indeed, when using supply ventilation systems, the air blown into the building can be filtered and preheated during the heating season, thus improving indoor air quality and providing thermal comfort in efficient buildings (Rahmeh, 2014).

## 2. A solar thermal system producing DHW and preheating the ventilation air

### 2.1. Presentation of the studied system

The studied solar system produces DHW, by heating the cold water (CW) that enters the tank, and preheats the ventilation air regarding the scheme in Fig. 1. To do this, the heat transfer fluid flowing in the solar loop delivers the collected solar energy into the storage tank by using the C1 circulator or directly to the air in the hot water coil with the C2 circulator. During the periods where solar energy cannot be collected, the air can also be preheated by using the stored energy if needed. In this case, a three-way valve (V3V) allows the fluid to change its flowing path through the heat exchanger in the tank first and then through the hot water coil. Both in the storage tank as well as in the


doi:10.18086/eurosun2018.01.03 Available at http://proceedings.ises.org

supply air flow, auxiliary heaters, $Aux_{Sto}$ and $Aux_{Air}$, may be needed to reach the respective set point temperatures of the tank ($T_{SetSto}$) and of the preheated air ($T_{SetAir}$). The preheating temperature $T_{SetAir}$ is set so that thermal comfort is guaranteed during the heating season.

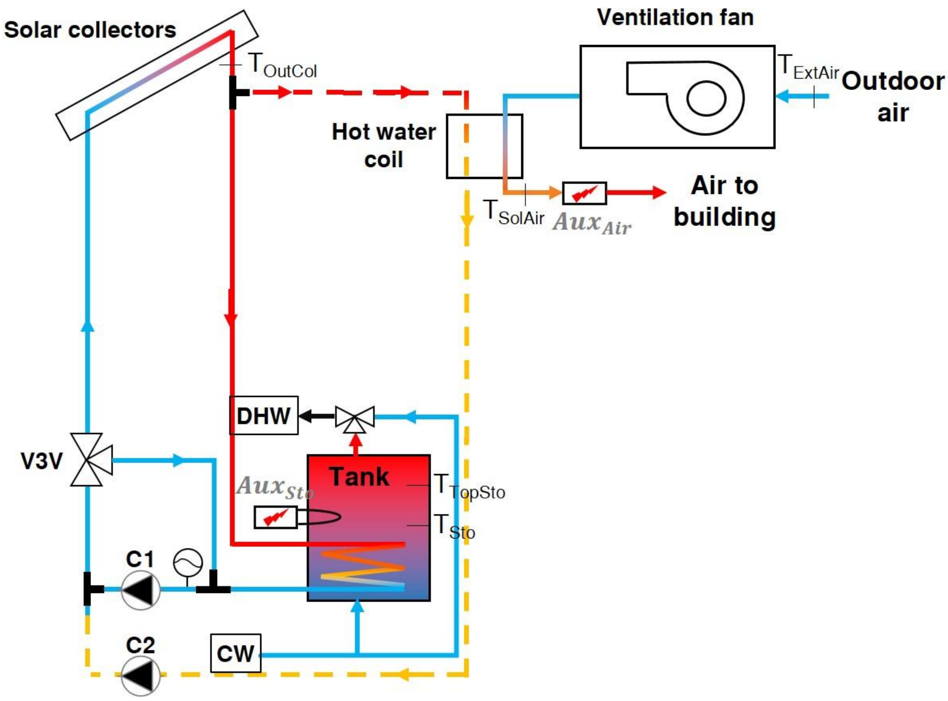


**Fig. 1. Scheme of the studied solar thermal system for DHW production and ventilation air preheating.**

## 2.2. Control algorithm

Solar energy distribution

Tab. 1 represents the algorithm for distributing the collected solar energy in the storage tank and/or the hot water coil by controlling the 3-way valve (V3V), the C1 and the C2 circulators. The rows in Tab. 1 describe the different conditions used in the control algorithm. The last four columns correspond to the four possible operation modes of the system, which are activated if the conditions of the respective column are fulfilled. The temperatures needed for control are represented in Fig. 1.

First, the orientation of the 3-way valve (V3V) is defined. On the one hand, if the solar energy can be collected and either stored in the tank or used immediately to heat the air in the hot water coil, the V3V guides the heat transfer fluid through the solar collectors. Then, if the collected solar energy is enough for heating the tank and if the temperature of the stored water is lower than its maximal temperature $T_{MaxSto}$, the C1 circulator is switched on. At the same time, during the season where air preheating is appropriate, if the outdoor air temperature $T_{ExtAir}$ is lower than the set air temperature $T_{SetAir}$ and if solar energy can heat the air, the C2 circulator is turned on, controlling that the air temperature $T_{SolAir}$ is under its maximal temperature $T_{MaxAir}$. The DT1 and DT2 parameters represent the threshold for defining if the collected energy is enough for heating the tank or the air respectively, and both include hysteresis. The « Heating_Season » function defines the necessity of air preheating regarding the average outdoor air temperature over 4 weeks $\bar{T}_{ExtAir}$. The end of the preheating season is defined when the average outdoor temperature $\bar{T}_{ExtAir}$ is over 15°C and the beginning when $\bar{T}_{ExtAir}$ is below 12°C .

On the other hand, if it is not appropriate to circulate the heat transfer fluid through the solar collectors, the V3V is oriented towards the submerged heat exchanger in the tank, allowing the air to be preheated by using the stored energy. The C2 circulator is then switched on during the heating season if the tank temperature is higher than a minimal temperature $T_{MinStoAir}$ and higher than the outdoor air temperature $T_{ExtAir}$, keeping the preheated air temperature under the limit temperature $T_{MaxAir}$.

Supplied auxiliary energy

The auxiliary systems in the tank, in the air flow as well as in the building for covering the space heating demand, are switched on if the respective set point temperatures $T_{SetSto}$, $T_{SetAir}$ and $T_{SetBuil}$ are not reached. The auxiliary heater in the tank works the whole year while the auxiliary systems concerning the air flow and space heating are only used during the heating season.

**Tab. 1. Control algorithm defining the solar energy distribution between the storage tank and air preheating in simulation.**

<table>
<tr><th colspan="2" rowspan="2"></th><th colspan="3">V3V towards collectors</th><th>V3V towards tank</th></tr>
<tr><th colspan="2">C1 ON</th><th colspan="2">C1 OFF</th></tr>
<tr><th>Conditions</th><th>Meaning</th><th>C2 OFF</th><th colspan="3">C2 ON</th></tr>
<tr><td>$T_{OutCol} - T_{Sto} > DT1$</td><td>Enough solar energy is available for heating the stored water.</td><td>TRUE</td><td>TRUE</td><td rowspan="2">ONE OR MORE FALSE</td><td rowspan="2">ONE OR MORE FALSE</td></tr>
<tr><td>$T_{TopSto} < T_{MaxSto}$</td><td>The temperature of the water in the tank is lower than its maximal temperature $T_{MaxSto}$.</td><td>TRUE</td><td>TRUE</td></tr>
<tr><td>$T_{OutCol} - T_{ExtAir} > DT2$</td><td>Enough solar energy is available for heating the air in the coil.</td><td rowspan="3">ONE OR MORE FALSE</td><td>TRUE</td><td>TRUE</td><td>FALSE</td></tr>
<tr><td>$Heating\_Season$</td><td>The period is defined as cold, involving air preheating and space heating.</td><td>TRUE</td><td>TRUE</td><td>TRUE</td></tr>
<tr><td>$T_{ExtAir} < T_{SetAir}$</td><td>The outdoor air temperature is under the set point temperature $T_{SetAir}$.</td><td>TRUE</td><td>TRUE</td><td>TRUE</td></tr>
<tr><td>$T_{SolAir} < T_{MaxAir}$</td><td>The temperature of the preheated air $T_{SolAir}$ is under its maximal temperature $T_{MaxAir}$.</td><td>TRUE OR FALSE</td><td>TRUE OR FALSE</td><td>TRUE OR FALSE</td><td>TRUE</td></tr>
<tr><td>$T_{Sto} > T_{MinStoAir}$<br>AND<br>$T_{Sto} > T_{ExtAir}$</td><td>The energy stored in the tank is over a limit defined by a threshold temperature $T_{MinStoAir}$ and is enough for heating outdoor air.</td><td>TRUE OR FALSE</td><td>TRUE OR FALSE</td><td>TRUE OR FALSE</td><td>TRUE</td></tr>
</table>

## 3. Model development

### 3.1. Modelling the system

The innovative solar system as well as the control algorithm are modelled using the Modelica language in the Dymola environment. The acausal and object-oriented features of the Modelica language are well-adapted to multiphysical model development in buildings (Wetter et al., 2016). The involved components in the modelling come from the « Buildings » library, the « Modelica » library or from the works of Bois (2017). The Dassl solver is used in Dymola, keeping a variable time step during the simulation.

### 3.2. Parameters characterising the main components

Hot water coil

The parameters characterising the hot water coil are experimentally calibrated under real conditions. A solar thermal system for DHW production and air preheating was installed in a test house located in the INCAS platform at CEA INES (Le Bourget-du-Lac, France). The heat exchanger between the fresh air flow and the heat transfer fluid is the BTC-C-160 model from Tuvaco, a cross-flow heat exchanger. The heat transfer fluid is a mix between water (75% vol.) and mono-propylene glycol (25% vol.). The temperatures of the air and the heat transfer fluid are measured at the inlet and outlet of the hot water coil.

Numerically, the model *Fluid.HeatExchangers.DryEffectivenessNTU* from the « Buildings » library is used for representing the heat exchanger. The experimental air flow, heat transfer fluid flow and inlet temperatures of the air and of the water/glycol mixture constitute the inputs of the model. The standard deviation between the experimental and numerical air temperatures at the coil outlet is minimised for calibration by using Brent's algorithm from 6 to 12 April 2018. The value of the standard deviation is 0,68 K for the studied period. The delivered energy to the air in the exchanger is 3,03 kWh experimentally and 3,07 kWh numerically, obtaining a difference of 1,3% in the same period. Only the nominal inlet temperature is calibrated, the other parameters come from the data sheet. Tab. 2 presents all the parameters used in simulation.

**Tab. 2. Parameters involved in the modelling of the hot water coil.**

| | |
|---|---|
| **Nominal power (W)** | 1500 |
| **Nominal air flow ($m^3 \cdot s^{-1}$)** | 0,11 |
| **Nominal air inlet temperature (°C)** | 20 |
| **Nominal heat transfer fluid flow ($litre \cdot s^{-1}$)** | 0,018 |
| **Nominal heat transfer fluid inlet temperature (°C)** | 70 |

*Storage tank*

Similarly, the parameters characterising the model of the storage tank are obtained from the data sheet. Only the ratio between the external and internal convective coefficients (r) is experimentally calibrated under real conditions. The tank used is the SC1Z model from SolisArt, with a volume of 400 litres. The heat exchanger fluid is also a mix between water and mono-propylene glycol. The temperature of the heat transfer fluid is measured at the inlet and outlet of the submerged heat exchanger as well as the temperature of the hot water leaving the tank.

The model representing the tank is the component *Storage.StratifiedEnhancedInternalHex* from the « Buildings » library. The heat transfer fluid and the water flow rates as well as the inlet heat transfer fluid and water temperatures are the inputs for calibration. The standard deviation between the experimental and numerical temperature of the water leaving the tank is minimised with Brent's algorithm from 16 to 22 June 2018. All the water contained in the tank was renewed with cold water on the $15^{th}$ of June in order to set the initial conditions of the tank in the simulation. The standard deviation between the experimental and numerical hot water temperatures is 0,40 K for the studied period. The energy delivered by the heat transfer fluid to the water in the tank is 25,04 kWh experimentally and 24,14 kWh numerically, obtaining a difference of 3,6%. The parameters involved in tank modelling are shown in Tab. 3.

**Tab. 3. Parameters involved in the modelling of the 400-litre storage tank.**

| | |
|---|---|
| **Height without isolation (m)** | 1,56 |
| **Thickness of the isolation (m)** | 0,055 |
| **Thermal conductivity of the isolation ($W \cdot m^{-1} \cdot K^{-1}$)** | 0,023 |
| **Number of layers** | 20 |
| **Lower heat exchanger position (m)** | 0,305 |
| **Upper heat exchanger position (m)** | 0,860 |
| **Nominal power (W)** | 53000 |
| **Tank nominal temperature (°C)** | 10 |
| **Heat transfer fluid nominal temperature (°C)** | 80 |
| **Heat transfer fluid nominal mass flow rate ($kg \cdot s^{-1}$)** | 0,37 |
| **Ratio between the external and internal convective coefficients for the heat exchanger (r)** | 0,34 |

*Solar collectors*

The component *Fluid.SolarCollectors.EN12975* from the « Buildings » library is used for modelling the solar collectors following the European test standard EN 12975. The parameters of a generic collector defined in Task 32 of the IEA (Heimrath and Haller, 2007), shown in Tab. 4, are used in simulations.

**Tab. 4. Parameters involved in the modelling of solar collectors.**

| | |
|---|---|
| **Optical efficiency $\eta_0$** | 0,8 |
| **Loss coefficient $a_1$ ($W \cdot m^{-2} \cdot K^{-1}$)** | 3,5 |
| **Loss coefficient $a_2$ ($W \cdot m^{-2} \cdot K^{-2}$)** | 0,015 |
| **Incident angle modifier over the direct radiation $b_0$** | 0,18 |
| **Incident angle modifier over the diffuse radiation $K_{0,dif}$** | 0,9 |

### 3.3. A co-simulation for coupling the system model to the building model

Although Modelica is well-adapted to complex model development, a well-known and robust program as EnergyPlus (Crawley et al., 2001) is appropriate for building modelling, offering a good compromise between the detailed description of the envelope and the computation time when predicting heating needs. Consequently, the system model developed with the Modelica language is coupled to a building model using EnergyPlus with a co-simulation. Indeed, a « Functional Mockup Interface » (FMI) (Blochwitz et al., 2011) is created, meaning that the building model is encapsulated as a « Functional Mockup Unit » (FMU) and imported into Dymola. The communication time step is 10 minutes, corresponding to the EnergyPlus constant time step used for the building simulation. The air flow rate and the preheated air temperature are sent to the building model, while the system model receives the indoor temperatures of the house. The computing time for simulating one year is 27 minutes with a Intel Xeon processor W3520 (2,66 GHz and 16 GB RAM).

The modelled building is the test house where the real system used for calibration was installed, which is a low-energy individual house. The inside dimensions are 7,5 m x 6,5 m, with a height under ceiling of 2,7 m in the ground floor and 2,4 m in the first floor, obtaining a living area of 89 $m^2$. The model considers four thermal zones (basement, ground floor, first floor and roofspace), where only the ground and first floors are heated areas. Ventilation air is supplied in two points: one in the ground floor and the other in the first floor. The used scenario for internal heat gains and occupancy considering a 4-person family come from the PhD thesis of Spitz (2012).

## 4. Numerical study

This section presents the numerical study of the innovative solar thermal system producing DHW and preheating the ventilation air, and is compared to a classical solar domestic hot water (SDHW) system.

### 4.1. Hypothesis

<u>Studied climates</u>
Seven French cities are studied: Bordeaux, Brest, Lyon, Marseille, Nantes, Paris and Strasbourg. The weather files used for simulation are obtained from the EnergyPlus database. The main variables of these files are summarized in Tab. 5, characterizing the weather conditions of each studied city as well as the air preheating period obtained from the « Heating_Season » function defined in Tab. 1.

**Tab. 5. Minimal, maximal and average temperature (T), global horizontal radiation (GHI), direct normal radiation (BNI), diffuse horizontal radiation (DHI) and simulated heating period for the studied climates in a typical year.**

| | Bordeaux | Brest | Lyon | Marseille | Nantes | Paris | Strasbourg |
|---|---|---|---|---|---|---|---|
| **Minimal T (ºC)** | -8,2 | -4,0 | -8,5 | -4,0 | -5,3 | -6,0 | -9,6 |
| **Maximal T (ºC)** | 34,0 | 29 | 33,6 | 34 | 32 | 30 | 31 |
| **Average T (ºC)** | 13,2 | 11,2 | 11,9 | 14,8 | 12,2 | 11,1 | 10,3 |
| **GHI ($kWh \cdot m^{-2}$)** | 1264,6 | 1085,4 | 1203,5 | 1545,4 | 1184,1 | 1068,1 | 1091,1 |
| **BNI ($kWh \cdot m^{-2}$)** | 929,9 | 661,3 | 861,5 | 1503,8 | 885,4 | 678,9 | 721,9 |
| **DHI ($kWh \cdot m^{-2}$)** | 712,0 | 688,5 | 666,2 | 615,4 | 665,1 | 668,8 | 650,4 |
| **Preheating start** | Late Oct | Mid-Oct | Mid-Oct | Early Nov | Late Oct | Early Oct | Early Oct |
| **Preheating end** | Mid-May | Late June | Mid-May | Late April | Late May | Late May | Late May |

<u>Control variables</u>
The control variables used in simulation, appearing in section 2.2, are presented in Tab. 6. The two values of the DT1 and DT2 parameters represent the bottom and upper limits of the hysteresis. The maximal air temperature of 50 °C is defined in order to avoid the risk of dust carbonization in the air, which is dangerous for health (Feist et al., 2005).

<u>Design parameters</u>
The collector surface used in the modelling is 4 $m^2$ for all the studied climates, the collectors having an inclination of 33°. The tank has a volume of 400 litres and the ventilation air flow is set to 0,0375 $m^3 \cdot s^{-1}$ (135 $m^3 \cdot h^{-1}$). The domestic hot water (DHW) demand is set to 200 litres per day at 45°C for a 4-person family. The water drawing pattern is obtained from Task 26 (Jordan and Vajen, 2000) with a 1-hour time step.

**Tab. 6. Values of the parameters involved in the control algorithm in simulation.**

| | |
|---|---|
| **Temperature differential for activating the C1 circulator DT1 (K)** | 4-10 |
| **Temperature differential for activating the C2 circulation DT2 (K)** | 2-6 |
| **Maximal water temperature allowed in the tank $T_{MaxSto}$ (°C)** | 90 |
| **Maximal air temperature allowed $T_{MaxAir}$** | 50 |
| **Minimal water temperature in the tank for air preheating $T_{MinStoAir}$ (°C)** | 30 |
| **Set point temperature for water stored in the upper part of the tank $T_{SetSto}$ (°C)** | 55 |
| **Set point temperature for air preheating $T_{SetAir}$ (°C)** | 15 |
| **Set point temperature in the building $T_{SetBuil}$ (°C)** | Occupation: 19<br>No occupation: 16 |

## *4.2. Performance indicators*

The following indicators are defined in order to analyse the energetic behaviour of the studied solar system.

- Collector efficiency ($\eta_{Col}$): represents the ratio between the energy recovered by solar collectors and the radiation arriving to the total collector tilted surface.
- Solar productivity (SP): is defined as the collected solar energy per unit of collector surface, in kWh·m$^{-2}$.
- Storage efficiency ($\eta_{Sto}$): represents the ratio between the useful energy delivered by the storage tank and the total supplied energy (solar and auxiliary) to the tank.
- DHW solar fraction ($F_{DHW}$): represents the ratio between the useful solar energy participating in the DHW production and the DHW needs.
- Air preheating solar fraction ($F_{Air}$): represents the part of the heat needed to raise the fresh air temperature $T_{ExtAir}$ to the set point temperature $T_{SetAir}$ covered by the solar energy collected with the solar system.
- System solar fraction ($F_{System}$): represents the part of DHW and air preheating needs covered by the solar energy collected with the solar system.
- Global solar fraction ($F_T$): represents the part of DHW, air preheating and space heating needs covered by the solar energy collected with the solar system.

## *4.3. Annual performance results in Lyon*

The studied system is simulated and compared to the « reference » system, a typical solar domestic hot water (SDHW) heater where the set point temperature of the air is reached only by using the electric auxiliary heater in the air flow. Fig. 2 represents the annual indicators defined in the section 4.2.

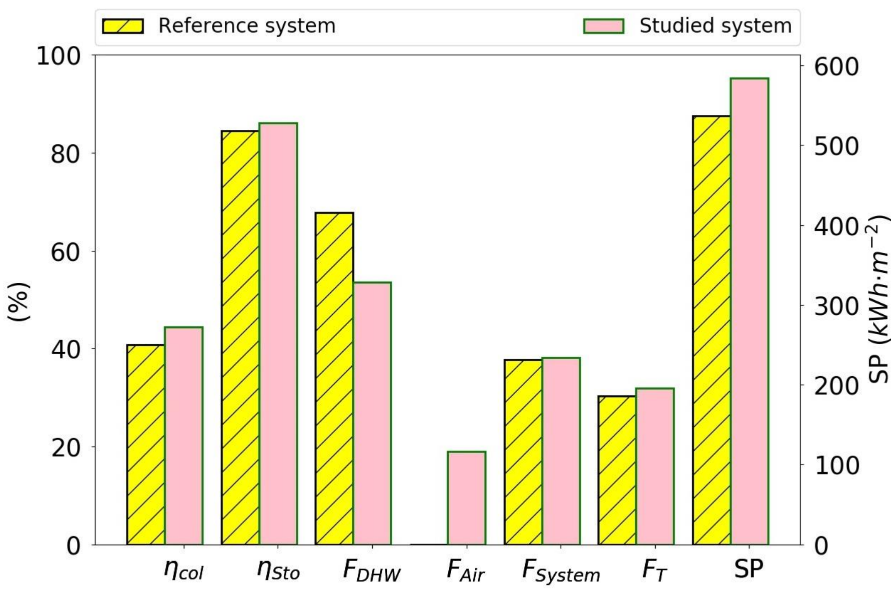


**Fig. 2: Annual performance indicators obtained numerically for the studied system producing DHW and preheating the ventilation air and compared to a classical SDHW heater (reference system), both coupled to the modelled building for the climate of Lyon.**

The collector efficiency $\eta_{Col}$ increases from 40,8% for the reference system to 44,3% for the innovative system since more solar energy can be collected thanks to air preheating, increasing the collector solar productivity SP by about 8,8%. The air preheated by using the energy stored in the tank leads to an improved tank efficiency $\eta_{Sto}$ since a part of the tank losses are converted into useful energy. Regarding solar fractions, since less solar energy is supplied for covering DHW needs, the DHW solar fraction $F_{DHW}$ decreases. On the contrary, a part of the total supplied energy to the air is covered by solar energy, increasing the air solar fraction $F_{Air}$. Nevertheless, the solar fraction of the system $F_{System}$ is almost the same in both cases, meaning that the auxiliary energy savings achieved in air preheating are needed for heating the tank. The additional solar energy recovered with the studied system is mostly used for heating the air over the set point temperature $T_{SetAir}$, decreasing space heating consumption. Thus, the global solar fraction increases from 30,3 % with the reference system to 31,9 % with the studied system.

Fig. 3 shows, on the one hand, the energy entering the storage tank as well as the hot water coil (IN) for the reference and the studied systems. On the other hand, the delivered energy uses (OUT) are presented. As explained before, the sum of the auxiliary energy consumption in the tank and in the air flow is almost the same for both cases. However, energy savings are achieved when considering space heating. The total energy delivered (OUT) is higher with the studied system due to air overheating.

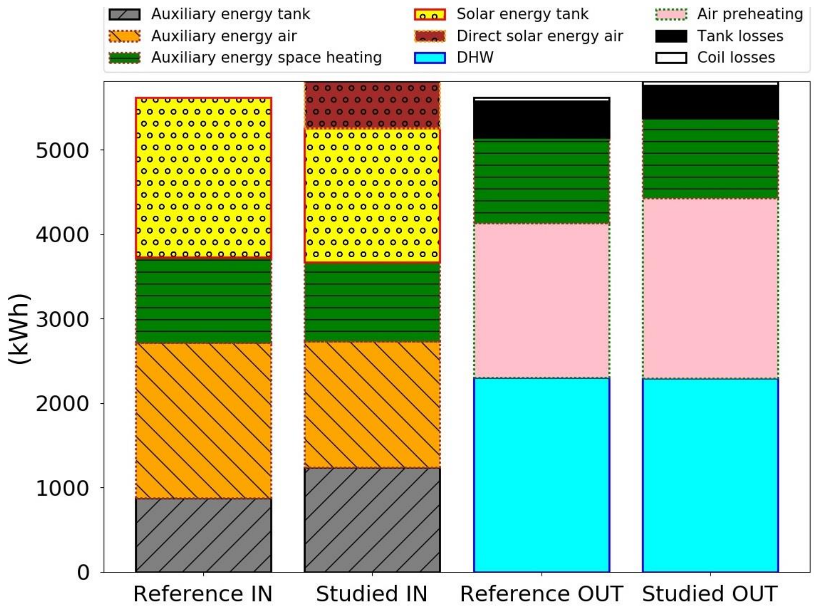


**Fig. 3. Annual solar and auxiliary energies supplied for covering the DHW, air preheating and space heating needs for the reference and the studied systems for the climate of Lyon.**

Fig. 4 shows a histogram of the temperature of the preheated air supplied to the building during the heating season for the studied and reference systems in order to illustrate air overheating when using the innovative system. The histogram of the outdoor air temperature during the heating season is also represented. Indeed, thermal comfort is improved when preheating the ventilation air by preventing cold air from blowing on the occupants. Fig. 4 also shows that the air is mostly preheated to the set point temperature $T_{SetAir}$ of 15°C for both systems but the studied system supplies a warmer air than the reference system during about 800 hours. A zoom of the air temperatures between -8 and 44°C shows closely the different distributions.

Higher supply air temperatures result in higher indoor temperatures for the studied system, as presented in Fig. 5. Consequently, the auxiliary energy consumption for space heating decreases about 6,5 % and the total auxiliary energy concerning DHW, air preheating and space heating also decreases about 1,5 % when using the innovative system, as shown before in Fig. 3. Indeed, air overheating is sometimes useful for reducing space heating consumption but, in other cases, it only increases indoor temperature when space heating is not needed, as shown in Fig. 5. For a building set point temperature of 19°C during occupation and 16°C with no occupation, temperatures in the ground floor are over 22°C for a longer time when using the innovative system. Fig. 5 also shows that air preheating provides a better thermal comfort, with higher indoor air temperatures, regarding a case without ventilation air preheating

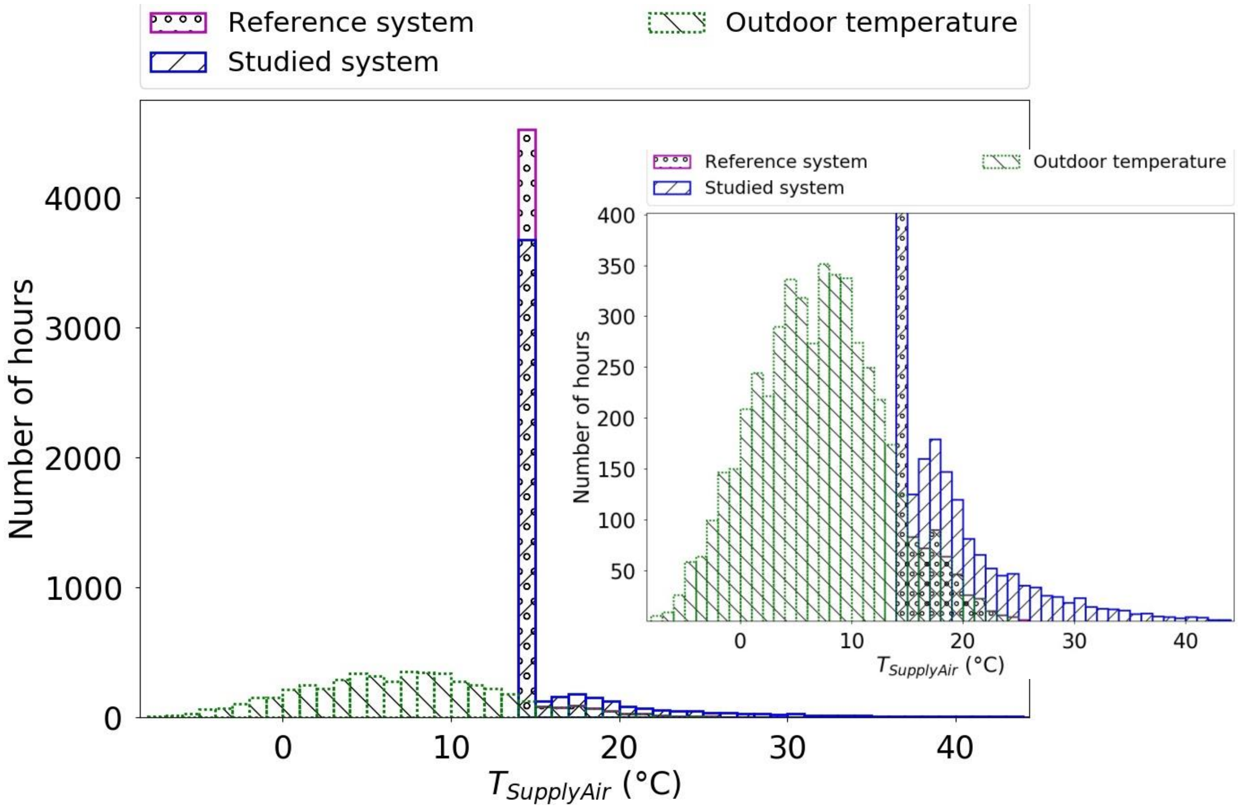


**Fig. 4. Histogram of the supply air temperature when using the reference or the studied system and outdoor temperature during the preheating season in Lyon, including a zoom for air temperatures between -8 and 44°C.**

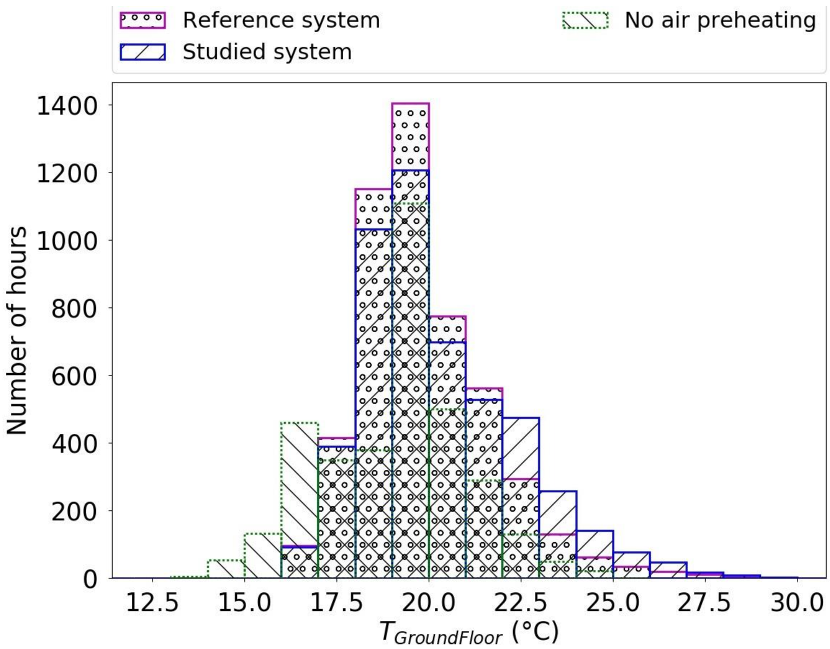


**Fig. 5. Histogram of indoor temperatures of the ground floor during the heating season for the studied and the reference systems as well as for a case without air preheating, for the climate of Lyon.**

## *4.4. Parametric analysis*

*Variation of the climate*

The innovative system is studied hereafter for the different climates introduced in section 4.1. Fig. 6 shows the solar productivity SP for the reference and the innovative systems depending on the climate. There is a significant increase of the SP in all the studied cities thanks to air preheating, the SP improvement varying from 12,0% in Paris to 22,3% in Brest, the latter presenting a longer period for air preheating (Tab. 5) which allows the system to collect a higher quantity of solar energy. Nevertheless, the auxiliary energy consumption for heating the tank and for preheating the air is higher for all the studied climates when using the studied system, with the exception of Strasbourg where this auxiliary energy consumption decreases about 1,1%. The auxiliary energy consumption used for DHW, air preheating and space heating is slightly reduced in the majority of climates with the innovative system, between 0,7 % in Brest and 2,3% in Strasbourg, except for the warmer climates, Bordeaux and Marseille, where the total auxiliary energy consumption increases. In these cases, even if more solar energy is collected with the innovative system as shown in Fig. 6, the additional solar energy is mostly used to overheat the building instead of producing DHW. Thus, solar energy must be better distributed with a different control strategy.

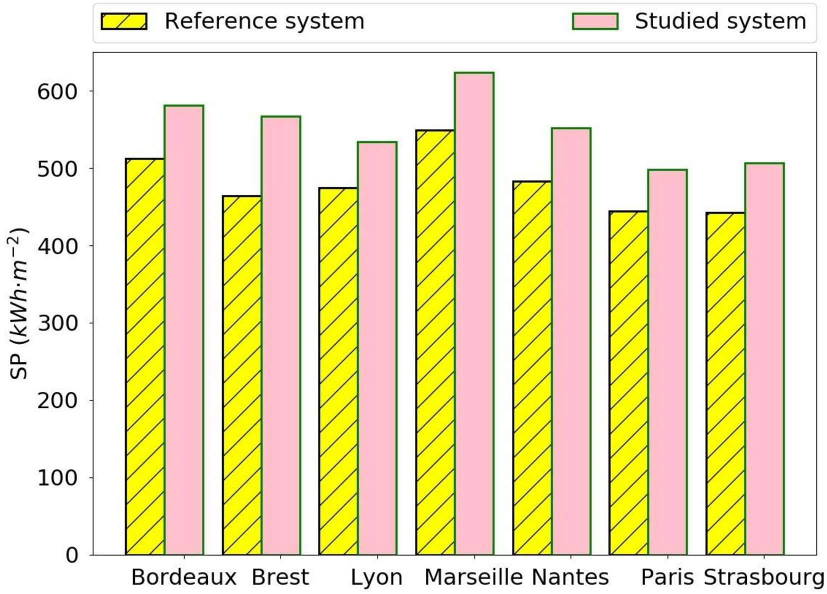


**Fig. 6. Annual comparison of the solar productivity SP for the reference system and the innovative systems depending on the climate.**

*Variation of the collector surface*

Collector surfaces ($S_{Col}$) from 2 to 10 m$^2$ are simulated for the climate of Lyon for the studied system. As shown in Fig. 7, the solar productivity SP decreases when increasing the collector surface. However, the global solar fraction $F_T$ increases with surface. Consequently, an important collector surface is more interesting from the energetic point of view, while keeping an appropriate solar productivity.

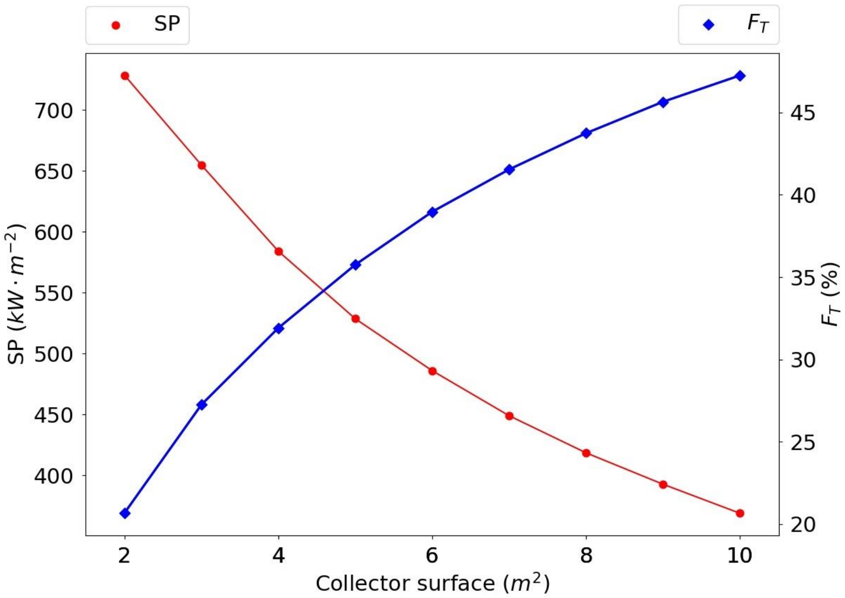


**Fig. 7. Annual USP and global solar fraction for the climate of Lyon when using the innovative system for different collector surfaces.**

*Variation of the tank volume*

Three tank volumes ($V_{Sto}$) of 300, 400 and 500 litres are simulated for the climate of Lyon. As the tank thermal losses are reduced when decreasing the tank volume, the storage efficiency $\eta_{Sto}$ is also reduced as observed in Fig. 8. The total auxiliary energy consumption for DHW production, air preheating and space heating does not vary significantly when changing the tank volume. Thus, the volume of 300 litres seems appropriate for collecting and using the solar energy arriving to a collector surface of 4 m$^2$, with less thermal losses and a lower price than bigger tanks.

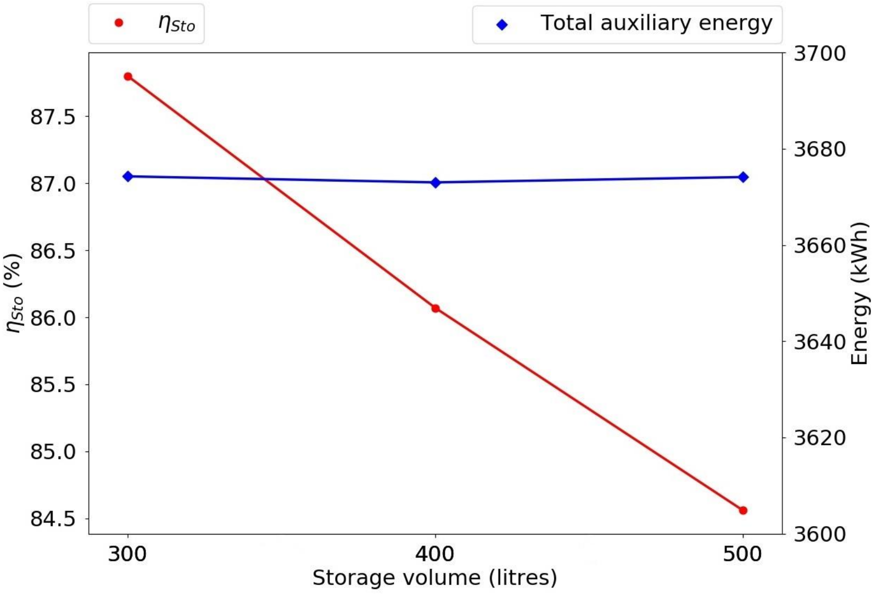


**Fig. 8. Annual storage efficiency and total auxiliary energy consumption for DHW production, air preheating and space heating for the climate of Lyon when using the innovative system with different storage volumes.**

<u>*Variation of the minimal temperature to enable air preheating with the stored energy*</u>

Five temperatures ($T_{MinStoAir}$): 10, 20, 30, 40 and 120°C are simulated for the studied system for the climate of Lyon and compared in Fig. 9. The case of 120°C represents a system where the air preheating by using the storage is not possible. The storage efficiency $\eta_{Sto}$ increases when decreasing $T_{MinStoAir}$, meaning that a part of the tank thermal losses are transformed into useful solar energy. Nevertheless, the air preheating by using the energy stored in the tank is not enhanced neither with the involved control algorithm nor with the selected collector surface of 4 $m^2$. Consequently, the differences in energy savings concerning the total auxiliary energy consumption are not significant. In any case, the lowest temperature of 10°C is recommended for improving the energetic performances of the system. DHW comfort was checked and it is not deteriorated for the different temperatures $T_{MinStoAir}$.

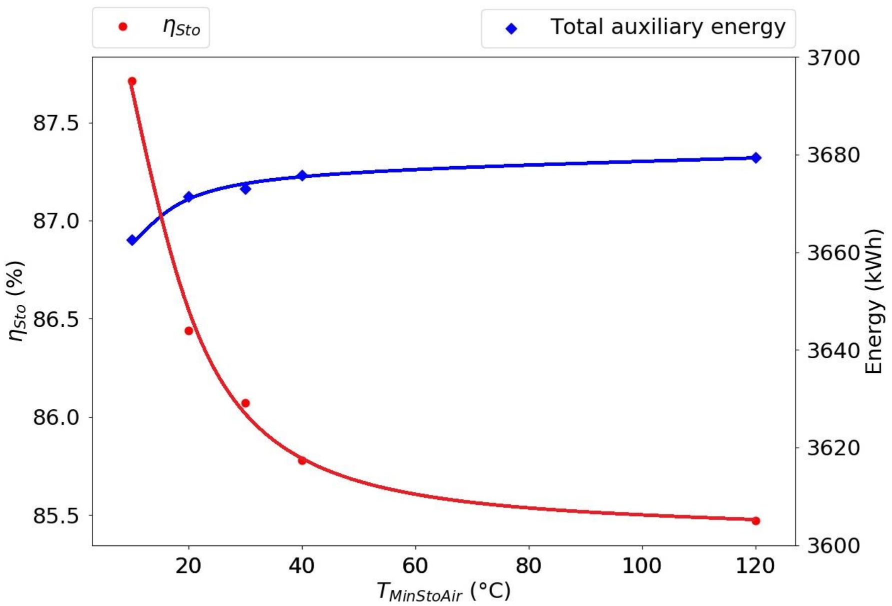


**Fig. 9. Annual storage efficiency and total auxiliary energy consumption for DHW production, air preheating and space heating for the climate of Lyon when using the innovative system with different minimal temperatures in the tank for allowing air preheating.**

<u>*Variation of the air preheating set temperature*</u>

Three set temperatures ($T_{SetAir}$ ) of 12, 15 and 18°C are simulated and compared for the climate of Lyon in Fig. 10. These values are the typical air preheating temperatures in France. Although a higher set air temperature $T_{SetAir}$ increases the solar productivity SP, the total auxiliary energy consumption for DHW production, air preheating and space heating also increases for a higher $T_{SetAir}$. Indeed, a higher set point temperature for air preheating requires outdoor air be preheated to a higher temperature, even when space heating is not necessary, thus increasing the total energy consumption. Consequently, the lower temperature $T_{SetAir}$ of 12°C is recommended.

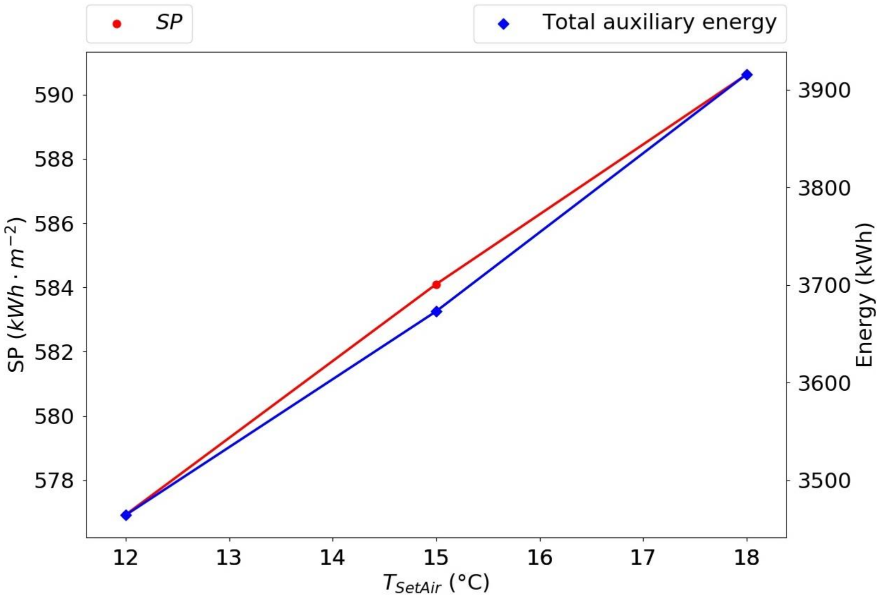


**Fig. 10. Annual solar productivity and total auxiliary energy consumption for DHW production, air preheating and space heating for the climate of Lyon when using the innovative system with different set air temperatures.**

## 5. Conclusions

This paper presents the numerical study of a solar thermal system producing DHW and preheating the ventilation air to a minimal temperature of 15°C, using a collector surface of 4 m$^2$ and a storage tank volume of 400 litres. The analysis is mainly done for the French city of Lyon, including the comparison with other French climates.

When comparing the innovative system with a classical SDHW system that only produces DHW, preheating the air with an independent auxiliary heater, the innovative system improves the collector efficiency and the solar productivity for all the studied climates. Thus, air preheating allows the system to collect and deliver more solar energy. Nevertheless, as part of the solar energy used for heating the storage tank in a classical SDHW system is now used for air preheating, more auxiliary energy must be supplied to the tank. Consequently, the auxiliary energy consumption for DHW production and for air preheating is increased for the majority of the studied climates when using the innovative system with a 4-m$^2$ collector surface and a 400-litre tank. This is due to air overheating, meaning that a significant part of the solar energy supplied to the air results in a temperature of the preheated air higher that its set point temperature $T_{SetAir}$, thus reducing the space heating energy consumption. Regarding the total auxiliary energy consumption for DHW production, air preheating and space heating, energy savings between 0,7 and 2,3 % are achieved depending on the climate, except for Bordeaux and Marseille, the warmer climates, where the total auxiliary energy consumption increases with the studied system. Consequently, particularly for the climates of Bordeaux and Marseille but also for the other climates where energy savings are not significant, the control strategy should enhance the storage of solar energy when air overheating is not useful for reducing space heating consumption. In general, when dimensioning the solar system for a typical DHW application, there is no much extra solar energy available for air preheating. Thus, the control algorithm is essential for optimising energy performance. Even if energy gains are limited, they are interesting as they can be achieved easily, only by adding a heat exchanger coupling the solar loop and the ventilation network.

Finally, a parametric analysis for the climate of Lyon provides some clues for improving the energy performance of the studied system. Increasing the collector surface results in a higher global solar fraction and a lower solar productivity. Thus, the collector surface can be increased while keeping an acceptable solar productivity. The studied tank volumes do not show a significant impact of the energy savings provided by the innovative system. Consequently, the lower studied volume of 300 litres is recommended in order to increase the tank efficiency and decrease its price. The system also allows the air to be preheated indirectly by using the energy stored in the tank. Although this option provides some energy savings regarding the case without indirect air preheating, the implemented control strategy do not deliver enough energy to the tank to obtain significant energy savings with a collector surface of 4 m$^2$. Finally, a higher set point temperature for air preheating $T_{SetAir}$ results in a higher total auxiliary energy consumption regarding DHW production, air preheating as well as space heating. Consequently, it is not recommended to increase the set point temperature $T_{SetAir}$.

The next step of this study consists in optimising the control algorithm of the presented innovative system in order to improve the solar energy distribution and so, energy performance. A previous sensitivity analysis will differentiate the most influential variables over the energy performance indicators that should be optimised.

## 6. References

ADEME, 2012. Feuille de route stratégique solaire thermique.

Blochwitz, T., Otter, M., Arnold, M., Bausch, C., Clauß, C., Elmqvist, H., Junghanns, A., Mauss, J., Monteiro, M., Neidhold, T., Neumerkel, D., Olsson, H., Peetz, J.–., Wolf, S., Gmbh, A.S., Berlin, Q., Scai, F., Augustin, S., 2011. The Functional Mockup Interface for Tool independent Exchange of Simulation Models, in: Proceedings of the 8th International Modelica Conference.

Bois, J., 2017. Aide à la conception de maisons à énergie positive à forte ouverture solaire (PhD thesis). Université de Bordeaux.

Crawley, D.B., Lawrie, L.K., Winkelmann, F.C., Buhl, W.F., Huang, Y.J., Pedersen, C.O., Strand, R.K., Liesen, R.J., Fisher, D.E., Witte, M.J., Glazer, J., 2001. EnergyPlus: creating a new-generation building energy simulation program. Energy and Buildings 33, 319–331.

European Commission, 2013. Energy, transport and environment indicators, 2013 edition. Publications Office of the European Union, Luxembourg.

Faninger, G., 2010. The potential of solar heat in the future energy system. Faculty for Interdisciplinary Research and Continuing Education, IFF-University of Klagenfurt, Austria 20.

Feist, W., Schnieders, J., Dorer, V., Haas, A., 2005. Re-inventing air heating: Convenient and comfortable within the frame of the Passive House concept. Energy and Buildings, Research That Inspires 125 Years of EMPA 37, 1186–1203.

Heimrath, R., Haller, M., 2007. Project Report A2 of Subtask A: The Reference Heating System, the Template Solar System (No. Task 32). IEA SHC.

IEA, 2012. Technology Roadmap Solar Heating and Cooling.

IEA-ETSAP, IRENA, 2015. Solar Heating and Cooling for Residential Applications.

Ionescu, C., Baracu, T., Vlad, G.-E., Necula, H., Badea, A., 2015. The historical evolution of the energy efficient buildings. Renewable and Sustainable Energy Reviews 49, 243–253.

Jordan, U., Vajen, K., 2000. Realistic Domestic Hot-Water Profiles in Different Time Scales (No. Task 26). IEA SHC, Universität Marburg, FB Physik, Marburg, Germany.

Rahmeh, M., 2014. Etude expérimentale et numérique des performances de la ventilation mécanique par insufflation : qualité de l’air intérieur dans les bâtiments résidentiels (Phd thesis). Université de La Rochelle.

Spitz, C., 2012. Analyse de la fiabilité des outils de simulation et des incertitudes de métrologie appliquée à l’efficacité énergétique des bâtiments (PhD thesis). Université de Grenoble.

Wetter, M., Bonvini, M., Nouidui, T.S., 2016. Equation-based languages – A new paradigm for building energy modeling, simulation and optimization. Energy and Buildings 117, 290–300.